NJC

Accepted Manuscript

This is an *Accepted Manuscript*, which has been through the Royal Society of Chemistry peer review process and has been accepted for publication.

Accepted Manuscripts are published online shortly after acceptance, before technical editing, formatting and proof reading. Using this free service, authors can make their results available to the community, in citable form, before we publish the edited article. We will replace this *Accepted Manuscript* with the edited and formatted *Advance Article* as soon as it is available.

You can find more information about *Accepted Manuscripts* in the Information for Authors.

Please note that technical editing may introduce minor changes to the text and/or graphics, which may alter content. The journal's standard Terms & Conditions and the Ethical guidelines still apply. In no event shall the Royal Society of Chemistry be held responsible for any errors or omissions in this *Accepted Manuscript* or any consequences arising from the use of any information it contains.

ROYAL SOCIETY OF CHEMISTRY

www.rsc.org/njc

Synthesis, crystal structure, DNA-binding studies of different coordinate binuclear silver (I) complexes with benzimidazole open-chain ether ligands

Huilu Wu*, Jiawen Zhang, Chengyong Chen, Han Zhang, Hongping Peng, Fei Wang and Zaihui Yang

School of Chemical and Biological Engineering, Lanzhou Jiaotong University, Lanzhou, Gansu, 730070, P. R. China

Abstract

Three new binuclear silver (I) complexes, namely $[Ag_2(Meobb)_2](pic)_2 \cdot 2H_2O$ (**1**), $[Ag_2(Etobb)_2(pic)](pic) \cdot (CH_3CN)$ (**2**) and $[Ag_2(Bobb)_2(pic)_2]$ (**3**), (Meobb = 1,3-bis(1-methylbenzimidazol-2-yl)-2-oxapropane, Etobb = 1,3-bis(1-ethylbenzimidazol-2-yl)-2-oxapropane, Bobb = 1,3-bis(1-benzylbenzimidazol-2-yl)-2-oxapropane, pic=picrate), have been synthesized and characterized by elemental analyses, IR spectra and X-ray single crystal diffraction. Complex **1** displays a $Ag_2(Etobb)_2$ dimeric structure. Each silver (I) ion is coordinated to two nitrogen atoms, which adopted a distorted linear configuration. In the complex **2**, the coordination environment of the silver (I) atoms is different. The Ag1 ion is coordinated in a T-shaped tri-coordinated geometry and the Ag2 should be best described as distorted tetrahedron. Complex **3** exhibits a discrete disilver metallacyclic framework. One silver atom (Ag1) is located in a distorted tetrahedral geometry, the other one silver atom (Ag2) is five-coordinated via two nitrogen atoms, oxygen atoms and the Ag1 to form a distorted square-based pyramidal configuration. The interactions of the three complexes with calf thymus DNA (CT-DNA) has been investigated by electronic absorption titration, fluorescent

* Corresponding author. Tel/fax: +86 13893117544.
E-mail address: wuhuilu@163.com (H.-L. Wu).

spectroscopy and viscosity measurements, and the modes of CT-DNA binding to the complexes have been proposed. The experimental results suggest that the silver (I) complexes bind to DNA in an intercalation mode, and their binding affinity for DNA follows the order **1**> **2** >**3**. The DNA-binding studies exhibit that the stereo-hindrance has a larger influence on the binding ability to DNA. The complex which has smaller stereo-hindrance will be stronger binding to DNA.

Keywords: Benimidazole open-chain ether; Silver (I) complex; Crystal structure; DNA-binding.

Introduction

During recent decades, the chemistry of the silver (I) complex is an active, thriving field which has attracted a great research interest [1-4]. As more and more silver (I) complexes have been reported, many of them were used in the field of luminescence, catalysis, conduction and anticancer agent [5-8]. As a representative d^{10} electronic configurational metal, silver (I) has a very flexible coordination sphere, which enables it to adopt coordination numbers ranging from 2 to 6,even 7 and 8, resulting in its coordination geometry varying from liner to T-shaped, tetragonal, square pyramidal and octahedral [9-11]. Another interesting features of silver (I) is apt to form the short Ag…Ag (argentophilicity), Ag…π and Ag-C interactions in the silver (I) coordination polymers as well as non-covalent supramolecular interactions with aromatic clouds such as π…π, CH…π and anion…π [12]. Moreover, the silver (I) has a high affinity towards heteroatom like N, O and S of the ligands [13]. Thereby, more and more ligands containing N and O atom have been synthesized, such as benzimidazole and their derivatives.

Benzimidazole and their derivatives have drawn significant attention as an important class of heterocyclic compounds in chemistry and pharmacology [14-17]. Benzimidazole is an important fragment in medicinal chemistry and plays very important roles in numerous pharmaceutical molecules with a wide range of biological properties. Plenty of compounds containing benzimidazole group have been reported to exhibit anticancer [18], antiviral [19], anti-inflammatory [20],

antimicrobial [21], antioxidant [22] and anticoagulant properties [23].

Therefore, the investigation into silver (I) complex with benzimidazole is becoming a very popular and interesting field. Nowaday, plenty of silver (I) complexs with benzimidazole have been developed, many of them exhibit wide-ranging antimicrobial activity [24], photoluminescence and catalytic properties [25-26] and the potential to form supramolecular aggregates through π…π stacking interaction and hydrogen bonding [27]. Based on our previous investigations on silver (I) complexes containing benzimidazole derivatives [28-29], in this paper, we wish to report the synthesis, characterization and DNA-binding activities of silver (I) complexes **1-3** with three different V-shape ligands.

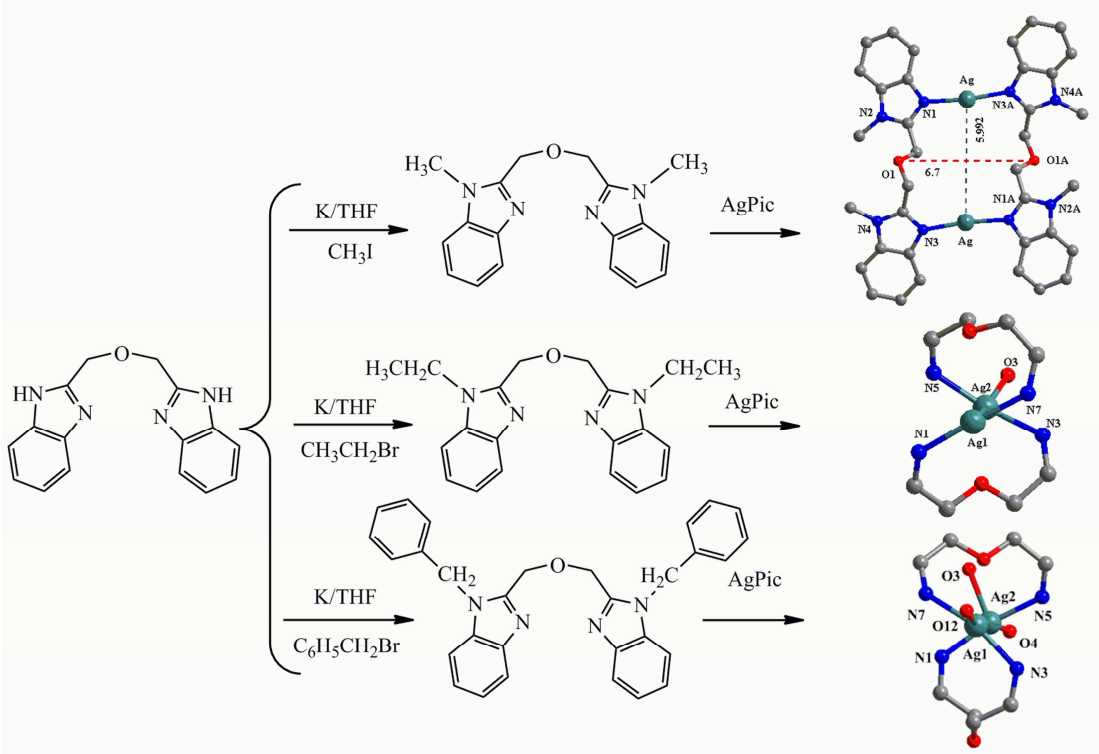

Scheme 1 Synthesis of complexes **1–3**.

Results and Discussion

Synthetic routes towards binuclear silver (I) complexes are exhibited in Scheme 1. The binuclear silver (I) complexes were obtained by reaction of Ag (pic) with three ligands Meobb, Etobb and Bobb in hot methanol. In contrast to silver (I) complexes, the three ligands are stable under atmospheric conditions. The silver (I) complexes are

remarkably soluble in polar aprotic solvents such as DMF, DMSO and MeCN; slightly soluble in water, ethanol, methanol, ethyl acetate and chloroform; insoluble in Et_2O and petroleum ether.

X-ray structure characterization

The structures of 1, 2 and 3 are confirmed by X-ray diffraction. The crystal structures are shown in Fig. 1, 4 and 5.

Crystal structure of 1.Crystallographic analysis reveals that complex **1** crystallizes in the triclinic space group P-1, and the structure of complex **1** displays an M_2L_2 dimeric structure, composed of a dinuclear $[Ag_2(Meobb)_2]^{2+}$ cation, two picrate anions and two aqua molecules. As seen from Fig. 1, two ligands are arranged in an end to end fashion to coordinate with two Ag (I) atoms. Each silver (I) ion is coordinated to two nitrogen atoms from two different Meobb ligands, forming a slightly distorted linear AgN_2 motif with an N1-Ag-N3 angle of 169.94°. It is noteworthy that this N1-Ag-N3 interaction as the ligand bridge. The $[Ag_2(Meobb)_2]^{2+}$ cation comprises a centrosymmetric binuclear pore canal structure through N1-Ag-N3 interaction (Fig. 1). The distance of the pore ranges from 5.992Å ($d_{Ag\text{-}Ag}$) to 6.7 Å ($d_{O1\text{-}O1A}$). The distance between the two silver (I) centres is 5.992Å, is much longer than the limit (2.91-3.24 Å) of those reported for weak Ag…Ag interaction in other silver (I) complexes [30-32], excluding any bonding interaction. It is obvious that two picrate anions do not participate in the coordination and only act as counter anions for charge equilibrium.

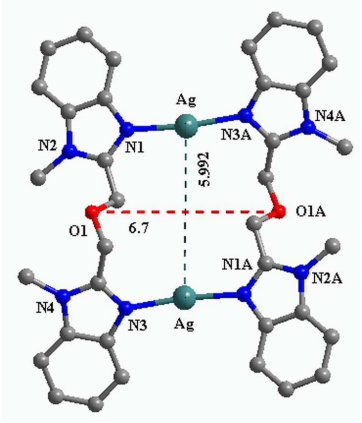

Fig. 1 The molecular structure of **1** with hydrogen atoms and picrate anions are omitted for clarity.

As depicted in Fig. 2. The $[Ag_2(Meobb)_2]^{2+}$ cation in crystalline $[Ag_2(Meobb)_2](pic)_2 \bullet 2H_2O$ piles up by strong π…π interaction between pairs of benzimidazole rings containing N3 and N4 (and symmetry related atoms), extending into a 1-D chain, the distance of the centroid-to-centroid between the two benzimidazole rings is 3.438Å. This type of interaction plays an important role in stabilization of the framework. It is greatly fascinating that two adjacent picrates anion and two aqua molecules are inlayed in the coordination cations as a sandwich and are connected by hydrogen bonds.

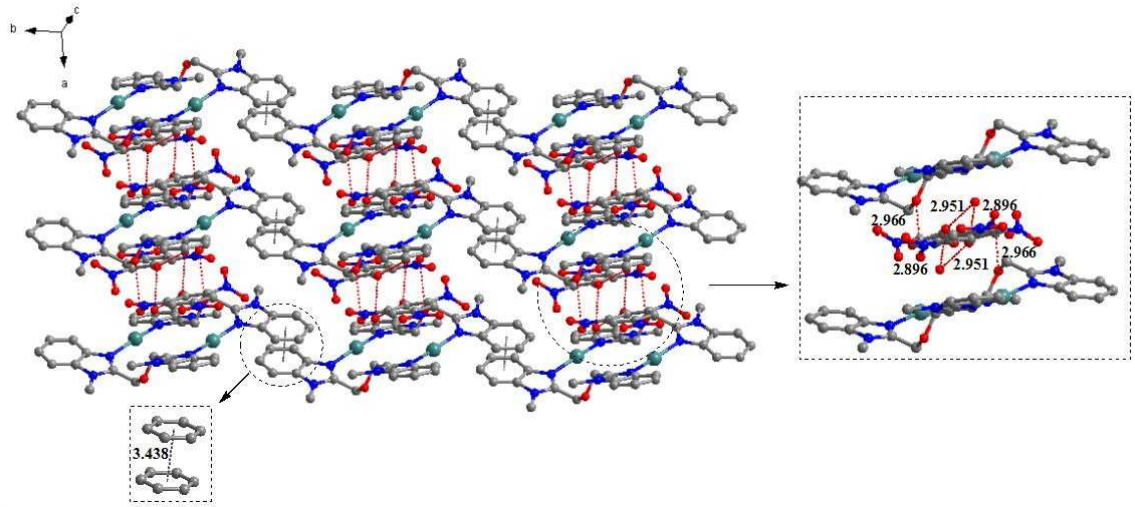

Fig. 2 A view of the packing in complex **1** showing the π···π stacking and hydrogen bonds between neighboring units.

The oxygen atoms of picrate anion and Meobb ligand are the strongest hydrogen bond acceptors and O-H groups of hydrone are the strongest hydrogen bond donors in the system [33]. O-H···O hydrogen bonds from hydrogen O-H to picrate, water and Meobb ligand are shown for structure $[Ag_2(Meobb)_2](pic)_2 \bullet H_2O$ in (Fig. 2). Owing to the existence of hydrogen bonds and the π…π stacking interaction, an infinite 2-D layer was created.

Crystal structure of 2. Single-crystal X-ray diffraction analysis reveals that complex **2** crystallizes in the triclinic space group P-1. The asymmetric unit of **2** is

composed of two silver (I) ions, two Etobb ligands and one picrate anion. The average N-Ag bond distance 2.127Å is similar to that in $\{[Ag(MeIm)_2](DNB)\}_2 \cdot H_2O$ (2.1196Å, MeIm = 2-methylimidazole, DNB = 3,5- dinitrobenzoate) [34], but longer than that in the complex **1** (2.106Å) and shorter than that in the complex **3** (2.155 Å). Carefully inspection of the crystal structure shows that the two silver (I) ions are coordinated differently, which there are three- and four-coordinate (Fig. 3). The coordination geometry around Ag1 ion is best described as T-shaped with the angle of N1-Ag1-N7 is 177.90°. The N3-Ag2-N5 angle (164.91°) is slightly deviated from linearity, but the coordination geometry around Ag2 should be best described as distorted tetrahedron considering the O3-Ag2 (2.526Å) and Ag1-Ag2 (2.997Å) interactions. The geometry for four-coordinate transition metal complex can be determined using the τ_4 geometry index, $\tau_4 = [360-(\alpha+\beta)]/141$, where α and β are the largest angles around metal center [35]. The four coordinate τ_4 values range from one for a perfect tetrahedral geometry to zero for perfect square planar geometry. The τ_4 parameter for Ag2 is 0.44 and it can be considered as slightly distorted seesaw geometry between tetrahedral geometry and square planar geometry. The Ag-Ag contacts lead to the dinuclear silver units of the complex, which are further bridged by the ligand to constructing two nine-membered rings and exhibiting an 8-shaped geometry (Fig. 3).

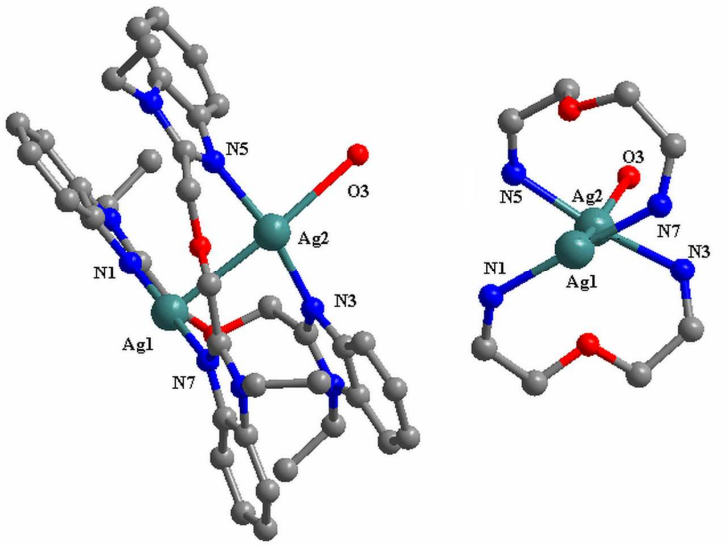

Fig. 3 The cation of complex **2** with H-atoms and uncoordinated picrate anion being

omited for clarity (left) and the 8-shaped geometric structure which is built by two nine-menbered rings (right).

Crystal structure of 3. The X-ray structural characterization shows that complex **3** belongs to the triclinic crystal system, crystallizing in space group P-1. As illustrated in (Fig. 4), in the complex **3**, the self-assembly of silver (I) ions and ligands gives the dinuclear $[Ag_2(Bobb)_2(pic)_2]$ motif. There are two silver (I) ions, which have different coordinate environment. The Ag1 ion adopts a distorted tetrahedron coordination geometry (τ_4 = [360-(α+β)]/141 = 0.21. herein, α = N(3)-Ag(1)-N(7)=163.5°, β = O(12)-Ag(1)-Ag(2) = 166.26°) with an oxygen atom (O12) from picrate group, two nitrogen atoms (N3, N7) from the two chelating Bobb ligands, respectively. However, the Ag2 center is five-coordinated via two nitrogen atoms (N5, N1), oxygen atoms (O3, O4) and the Ag1 to rarely distorted square-based pyramidal configuration. The parameter (τ_5) of five-coordinate geometry from a perfect trigonal bipyramidal geometry (τ_5 = 1) towards a regular square-based pyramidal (τ_5 = 0) has been calculated according to the method of Addison et al, τ_5 = (β-α) /60, where α and β are the largest angles around metal center [36]. The τ_5 parameter for Ag2 is 0.036 (herein β=O(4)-Ag(2)-Ag(1)=169.24°, α=N(1)-Ag(2)-N(5)=167.08°). The Ag1-Ag2 distance is 3.137 Å, which is significantly shorter than the sum of van der waals radii (3.44 Å), and is rather close to Ag-Ag distance in silver metal (3.048 Å) [37], indicating the presence of argentophilic interaction. The average O-Ag bond length 2.636 Å is longer than that in the complex 2 (2.526 Å). The Ag-Ag contacts result in the dinuclear silver units of the complex, which are further bridged by the ligand and construct two nine-membered rings which similar to the complex **2** (Fig. 3).

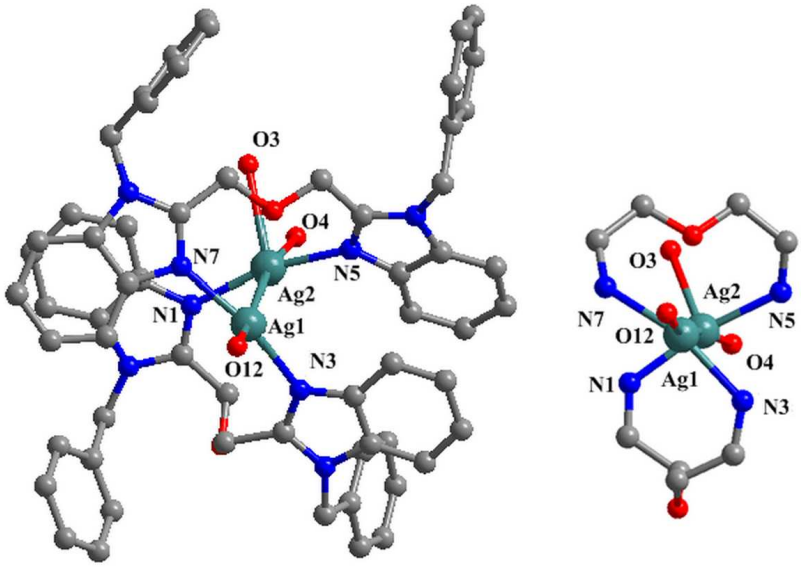

Fig. 4 The neutral unit and atom-labeling scheme of complex **3** (left) with hydrogen atoms and solvent molecule are omited for clarity. The 8-shaped geometric structure of complex **3** (right).

As one of important types of supramolecular forces, π···π stacking shows a specific structural requirement for substrate recognition or the arrangement of complicated architectures. In the complex **3**, the self-assembly of silver (I) ion and Bobb ligands generates the infinite 1-D chains, the asymmetry molecules are connected by benzimidazole rings π···π stacking interactions (Fig.5). The average centroid-to-centroid distance is 3.632 (1) Å.

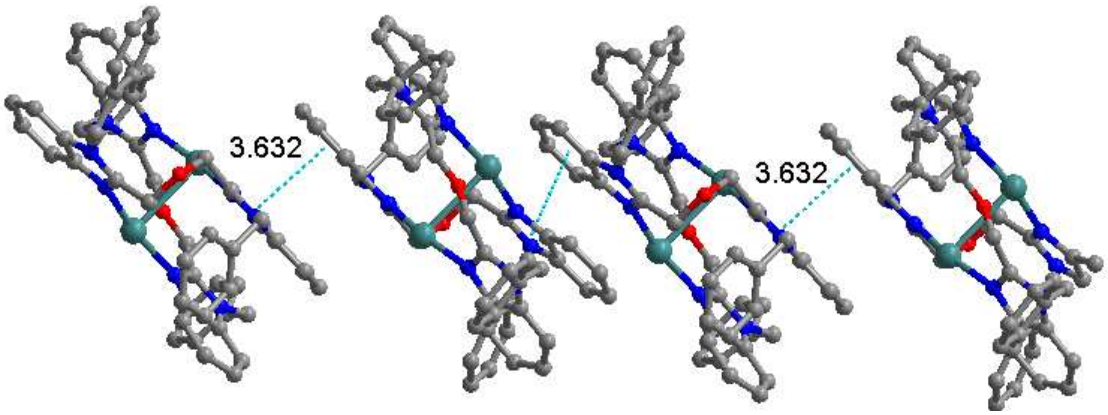

Fig.5 1-D chain of complex **3** by the benzimidazole ring π···π stacking.

In summary, three new binuclear silver (I) complexes were synthesized using three

ligands Meobb, Etobb and Bobb, and exhibit diverse intriguing structure. For complex **1**, two Meobb ligands were coordinated with two silver (I) atoms with two N1-Ag-N2 interactions, each silver (I) ion is two-coordinate. The major structure of complex **2** and complex **3** is similar and exhibit an 8-shaped geometric structure, but the coordination environment of the silver (I) atoms is different. In the complex **2**, the coordination numbers of two silver (I) atoms are three- and four-coordinate, while the coordination numbers of two silver (I) atoms are four-coordinate and five-coordinate in the complex **3.** By comparing the molecular structure of above-mentioned, the reason that the silver (I) complexes exhibit different structural conformation could be ascribed to different distortion and steric hindrance of the ligands.

DNA-binding studies

Electronic absorption titration.DNA-binding is the critical step for DNA cleavage in most cases. The application of electronic absorption spectroscopy in DNA-binding studies is one of the most useful techniques [38]. The binding of the metal complexes to DNA helix is often characterized through absorption spectral titration, followed by the changes in the absorbance and shift in the wavelength. To clarify the interaction between the complex and DNA, the absorption spectra of **1**-**3** in the absence and presence of CT-DNA are illustrated in Fig. 6a-c, respectively. These complexes exhibit intense absorption bands at 278-282 nm ascribed to $\pi\rightarrow\pi^*$ transition of benzimidazole and addition of increasing the concentration of CT-DNA most likely through the intercalative mode, because intercalation would lead to hypochromism and bathochromism in UV absorption spectra due to the intercalative mode involving a strong stacking interaction between an aromatic chromophore and the base pairs of DNA [39]. In the present case, with addition of DNA, three silver (I) complexes exhibit hypochromism of about 10.23%, 72.00% and 46.04% accompanied by bathochromism of about a 1-2 nm shift in the absorption maxima. The extent of the hypochromism is commonly consistent with the strength of intercalative interaction [40].

To compare the affinity of three Ag(I) complexes towards DNA, the intrinsic

binding constants K_b of the complex **1**, **2** and **3** are 2.26×10^5 M^{-1} (R^2=0.99 for 11 points), 1.09×10^5 M^{-1} (R^2=0.99 for 15 points) and 0.92×10^5 M^{-1} (R^2=0.99 for 12 points), respectively. The K_b values obtained here is lower than that reported for classical intercalator (for ethidium bromide) whose binding constants have been found to be 10^6 M^{-1} [41] and is three orders of magnitude more than our previous investigation on silver (I) complexes containing benzimidazole derivatives [29]. The results indicate that there is intercalative binding mode between the three complexes and CT-DNA. As can been seen from Fig. 6, the binding strength of complexes **1>2**>**3**. The reason for the difference in the binding strength for three Ag(I) complexes can attributed to the difference in steric hindrance, which are both caused by the introduction of substituents and geometric structure.

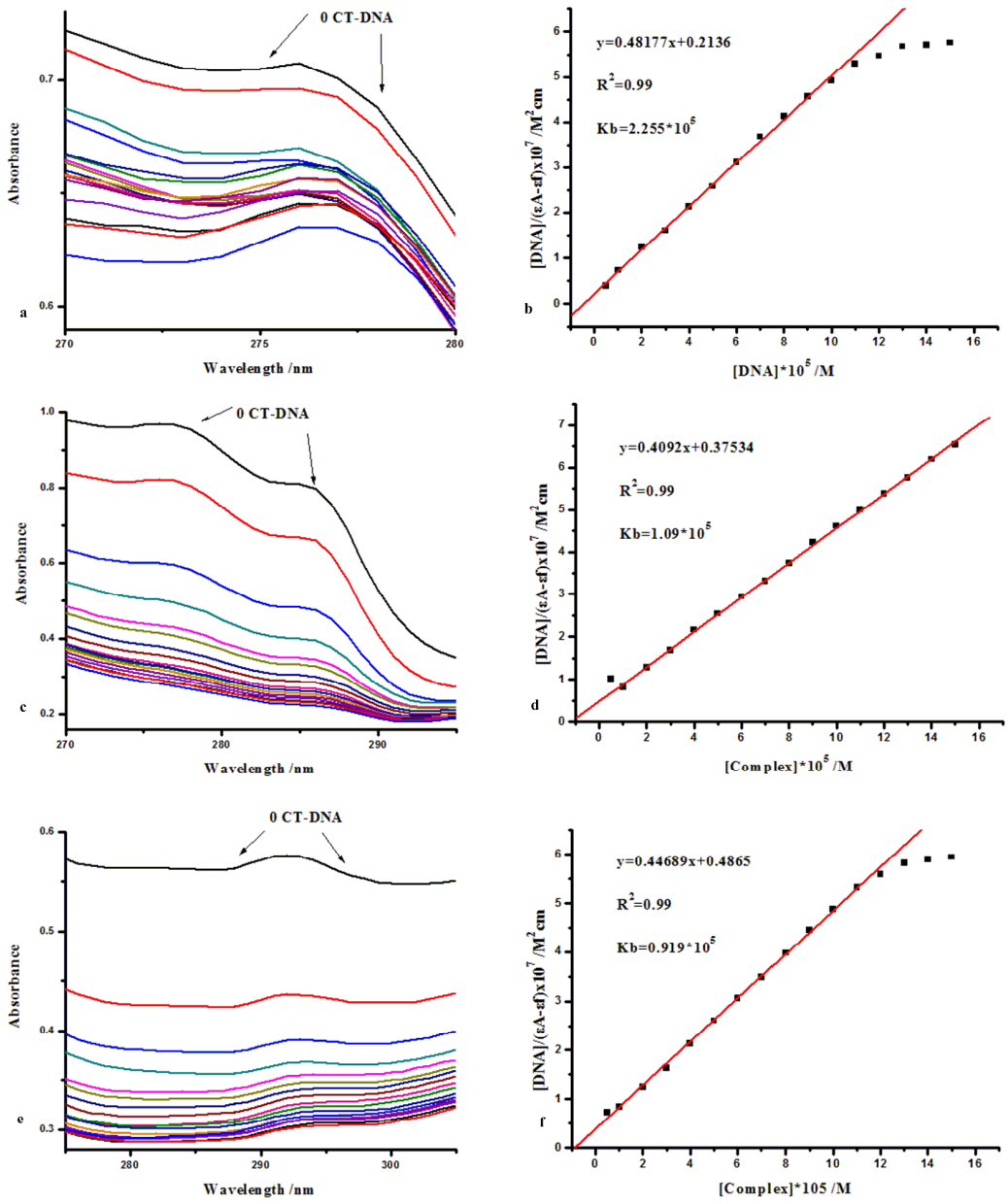

Fig. 6 Absorption spectral traces of (a) complex **1**, (c) complex **2** and (e) complex **3** in Tris-HCl buffer upon addition of CT-DNA. Arrows show the emission intensity changes upon increasing the DNA concentration. Plots of [DNA]/(ε_a - ε_f) vs. [DNA] for the titration of (b) complex **1**, (d) complex **2** and (f) complex **3** with CT-DNA. [Complex **1**], [complex **2**] and [complex **3**] = 2.0×10^{-5} mol/L , [DNA] = $0.5\text{-}9.0\times10^{-5}$ mol/L.

Fluorescence spectroscopic studies. No luminescence was observed for the complexes **1-3** at room temperature either in DMF or in the presence of CT-DNA. The binding of the complexes cannot be directly followed in the emission spectra. Hence,

steady state competitive binding studies of the three complexes are monitored by a fluorescent EB displacement assay. EB, a planar aromatic heterocyclic dye intercalates non-specially into the DNA which causes it to fluoresce strongly [42-43].

EB (weakfluorescent) + DNA (nonfluorescent) ↔ EB-DNA (strongfluorescent)

Thus, EB can be used to probe the interaction of the complexes with DNA. The relative binding of the complexes **1-3** to CT-DNA is studied with an EB-bound CT-DNA solution in 5mM Tris-HCl/50 mM NaCl buffer (PH=7.2) in Fig. 7. Fluorescence intensities (520 nm excitation) are measured at different complex concentrations. The emission intensity of DNA-EB system decreases appreciably, which indicated that the complexes could replace EB from the DNA-EB system. Such a characteristic change is often observed in intercalative binding modes [44]. As shown in Fig. 7, the quenching plot illustrates that the quenching of EB bound to DNA by complex is in agreement with the Stern-Volmer relationship, which also indicates the complex bind to DNA. The K_{sv} values for complexes **1-3** are found to be 7.95×10^4 (R^2=0.99 for 10 points), 4.36×10^4 (R^2=0.99 for 10 points) and 2.64×10^4 (R^2=0.98 for 8 points), respectively. The Stern-Volmer dynamic quenching constants can also be interpreted as binding affinities of the complexation reaction [45-46]. The K_{sv} values obtained here is similar to our previous work on silver (I) complexes containing benzimidazole derivatives [28]. And the binding ability to CT-DNA is that complex **1**>**2**>**3**. The result we obtained from the fluorescence spectrum is same as the absorption spectrum.

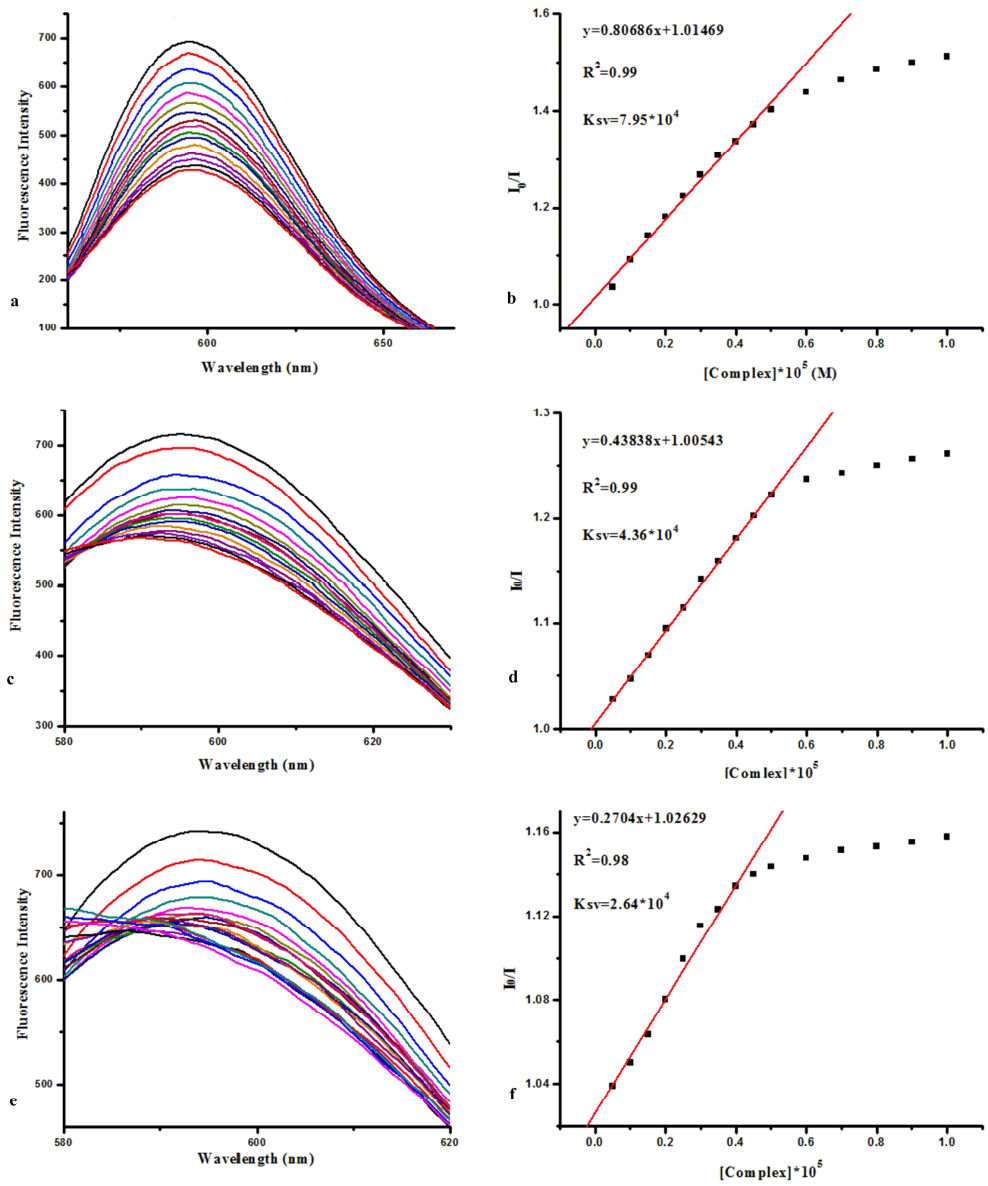

Fig. 7 Emission spectra of EB bound to DNA in the presence of (a) complex **1**, (c) complex **2** and (e) complex **3** in Tris-HCl buffer. Fluorescence quenching curves of EB bound to CT-DNA by (b) complex **1**, (d) complex **2** and (f) complex **3**. (Plots of I_0/I vs.[Complex]). [DNA]=2.5×10^{-3} mol/L; λ_{ex}=520 nm.

Viscosity measurements. Hydrodynamic measurements that are sensitive to changes in DNA length are considered as the least ambiguous and most critical tests of a binding model in solution in the absence of crystallographic data [47]. To further investigate the interaction properties between the metal complexes and DNA, the relative specific viscosity of DNA is examined by varying the concentration of the added metal complexes. Measuring the viscosity of DNA is a classical technique used

to analyze the DNA binding mode in solution [48]. A classical intercalative mode causes significant increase in viscosity of the DNA solution due to an increase in the separation of base pairs at the intercalation sites and hence an increase in overall DNA length. In contrast, complex that binds in the DNA grooves by partial and/or nonclassical intercalation cause less pronounced (positive or negative) or no change in DNA solution viscosity [49]. Fig. 8 depicts the effect of complexes **1-3** on the DNA viscosity. The results reveal that the complex **1**, **2** and **3** effect relatively apparent increase in DNA viscosity, which is consistent with DNA intercalative binding mode suggested above, which is also known to enhance DNA viscosity [50]. These results support that these complexes **1-3** bind to CT-DNA by intercalation [51].

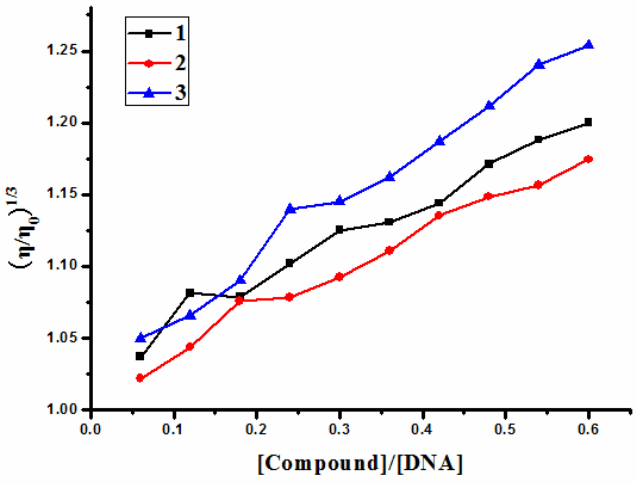

Fig.8 Effect of increasing amounts of the complexes on the relative viscosity of CT-DNA at 25.0 ± 0.1 °C.

Conclusions

In this paper, three benzimidazole open-chain ether ligands and their silver (I) complexes have been synthesized and characterized. In the complex 1-3, benzimidazole ligands all adopt the μ_2-bridging mode to link two silver atoms, forming three different binuclear motifs. Complex 2 and 3 display an obvious Ag-Ag contact. DNA-binding of the Ag(I) complexes suggest that three Ag (I) complexes bind to DNA in an intercalation mode, which is owing to the large planar aromatic rings, hydrogen bonds and π…π stacking interactions that facilitate them intercalating

into the base pairs of double helical DNA. Furthermore, the binding affinities of these Ag (I) complexes follow the order: 1>2>3. This result illustrates that steric hindrance plays a vital role in the DNA-binding of the three Ag (I) complexes. These studies suggest that Ag (I) complexes have potential practical applications in the development of potential probes of DNA structure and conformation and new therapeutic reagents for diseases on the molecular level and warrants further in vivo experiments and pharmacological assays.

Experimental

Caution: Although no problems are encountered in this work, transition-metal picrate salts are potentially explosive and should thus be prepared in small quantities and handled with care.

Materials and instrumentations

The Meobb, Etobb and Bobb ligands are synthesized according to the procedure [52]. Ethidium bromide (EB) and calf thymus DNA (CT-DNA) are purchased from Sigma Chemicals Co. (USA). Tris-HCl buffer solution is prepared using bidistilled water.

CHN elemental analyses were performed using a Carlo Erba 1106 elemental analyzer. IR spectra were recorded in the 4000-400 cm^{-1} regions with a Nicolet FT-VERTEX 70 spectrophotometer using on KBr pellets. The electronic spectra were measured on a Lab-Tech UV Bluestar spectrophotometer. The fluorescence spectral data were obtained on a 970-CRT fluorescence spectrophotometer at room temperature.

Synthesis

Three complexes were prepared using a similar procedure. The ligand (0.50mmol: Meobb, 153 mg; Etobb, 167 mg; Bobb, 229 mg) in hot MeOH (15 ml) is added silver(I) picrate (0.25 mmol, 84 mg) in MeOH (5 ml). A colorless crystalline product formed rapidly. The precipitate is filtered off, washed with MeOH and absolute Et_2O, and dried in *vacuo*. The product is dissolved in MeCN to form a colorless solution

that is allowed to evaporate at room temperature. The colorless crystals suitable for X-ray diffraction studies were obtained after several days.

Complex 1. Yield 71%. Anal. Calcd for $C_{48}H_{44}Ag_2N_{14}O_{18}$ (%): C, 43.61; H, 3.33; N, 14.84. Found (%): C, 44.02; H,3.35; N, 14.89. Selected IR data (KBr ν/cm^{-1}), 1084 ($\nu_{C\text{-}O\text{-}C}$), 1330 ($\nu_{NO_2}$), 1492 ($\nu_{C=N\text{-}C=C}$).

Complex 2. Yield 67%. Anal. Calcd for $C_{54}H_{51}Ag_2N_{15}O_{16}$ (%): C, 46.89; H, 3.69; N, 15.20. Found (%): C, 46.85; H, 3.71; N, 15.18. Selected IR data (KBr ν/cm^{-1}), 1078 ($\nu_{C\text{-}O\text{-}C}$), 1330 ($\nu_{NO_2}$), 1483 ($\nu_{C=N\text{-}C=C}$).

Complex 3. Yield 71%. Anal. Calcd for $C_{72}H_{56}Ag_2N_{14}O_{16}$ (%): C, 54.37; H, 3.52; N, 12.33. Found (%): C, 54.35; H, 3.61; N, 12.14. Selected IR data (KBr ν/cm^{-1}), 1068 ($\nu_{C\text{-}O\text{-}C}$), 1330 ($\nu_{NO_2}$), 1471 ($\nu_{C=N\text{-}C=C}$).

Table 1 Crystallographic data and structure refinement parameters for complexes **1**–**3**.

Complex	**1**	**2**	**3**
Empirical formula	$C_{48}H_{44}Ag_2N_{14}O_{18}$	$C_{54}H_{51}Ag_2N_{15}O_{16}$	$C_{72}H_{56}Ag_2N_{14}O_{16}$
Mr	1320.71	1381.84	1589.05
Crystal system	Triclinic	Triclinic	Triclinic
Space group	P-1	P-1	P-1
a (Å)	7.09520(10)	11.7172(3)	13.3730(3)
b (Å)	12.8978(3)	11.9846(3)	14.8244(4)
c (Å)	15.0574(4)	20.1196(6)	17.3282(4)
α (°)	110.5830(10)	89.9760(10)	86.8670(10)
β (°)	102.7630(10)	81.0430(10)	89.7150(10)
γ (°)	97.5890(10)	79.8740(10)	87.8750(10)
V (Å^3)	1224.46(5)	2746.33(13)	3427.75(14)
Z, Dc (mg/m^3)	1, 1.791	2, 1.671	2, 1.540
μ (mm^{-1})	0.895	0.800	0.652
F (000)	668	1404	1616
θ Range (°)	3.02 - 27.48	3.00 - 27.48	3.04 - 25.50
Limiting indices, hkl	-8 to 9	-15 to 13	-16 to 16
	-16 to 16	-15 to 15	-17 to 17
	-19 to 19	-26 to 26	-20 to 20
Reflections collected	12128	26608	28124
Unique reflections	5602	12603	12762
R_{int}	0.0151	0.0350	0.0352
Goodness-of-fit on F^2	1.031	1.062	1.179
R1/wR2 [I > 2σ(I)]	0.0223/ 0.0731	0.0390/0.1120	0.0487/ 0.1228
R1/wR2 (all data)	0.0245/0.0781	0.0534/0.1248	0.0877/0.1900
Largest diff. peak, hole (e Å^{-3})	0.519 , -0.582	0.729, -0.950	1.618, -1.531

X-ray diffraction

For each complex, a suitable single crystal was mounted on glass fibers for data collection in a Bruker Smart CCD diffractometer with graphite-monochromated Mo-Kα radiation (λ=0.71073 Å) at 153 K. Date reduction and cell refinement are performed by using the SMART and SAINT programs [53]. The absorption corrections are carried out by the empirical method. The structure is solved by direct methods and refined by full-matrix least-squares against F^2 of data using SHELXTL software [54]. All H atoms are found in difference electron maps and are subsequently refined in a riding-model approximation with C-H distances ranging from 0.95 to 0.99 Å. Information concerning the crystallographic data collection and structure refinements is summarized in Table 1. The relevant bond lengths and angles are listed in Table 2.

Crystallographic data for complexes **1**–**3** have been deposited with the Cambridge Crystallographic Data Centre as supplementary publication CCDC reference numbers are 721073, 721072 and 1408501, respectively. Any inquiries relating to the data can be e-mailed to deposit@ccdc.cam.ac.uk.

Table 2 The relevant bond distances (Å) and angles (°) for complexes **1**–**3**.

Complex **1**			
Ag-N(1)	2.1088(16)	N(3)-Ag#1	2.1038(15)
Ag-N(3)#1	2.1038(15)		
C(9)-O(1)-C(8)	112.12(14)	C(1)-N(1)-Ag	123.11(13)
N(3)#1-Ag-N(1)	169.94(6)	C(7)-N(1)-Ag	129.50(13)
C(10)-N(3)-Ag#1	126.54(13)	C(16)-N(3)-Ag#1	126.57(13)
Complex **2**			
Ag(1)-N(1)	2.124(3)	Ag(1)-N(7)	2.134(3)
Ag(1)-Ag(2)	2.9973(4)	Ag(2)-N(3)	2.117(3)
Ag(2)-N(5)	2.134(3)	Ag(2)-O(3)	2.526(3)
N(1)-Ag(1)-N(7)	177.90(12)	N(1)-Ag(1)-Ag(2)	90.66(8)
N(7)-Ag(1)-Ag(2)	89.32(8)	N(3)-Ag(2)-N(5)	164.91(12)
N(3)-Ag(2)-O(3)	104.34(12)	N(5)-Ag(2)-O(3)	90.63(12)
N(3)-Ag(2)-Ag(1)	79.32(8)	N(5)-Ag(2)-Ag(1)	89.23(8)
O(3)-Ag(2)-Ag(1)	132.51(7)	C(41)-O(3)-Ag(2)	141.5(3)
Complex **3**			
Ag(1)-N(3)	2.166(5)	Ag(1)-N(7)	2.174(5)

Ag(1)-O(12)	2.551(4)	Ag(1)-Ag(2)	3.1365(7)
Ag(2)-N(1)	2.138(5)	Ag(2)-N(5)	2.145(5)
N(3)-Ag(1)-N(7)	163.5(2)	N(3)-Ag(1)-O(12)	103.15(17)
N(7)-Ag(1)-O(12)	85.46(18)	N(3)-Ag(1)-Ag(2)	86.16(13)
N(7)-Ag(1)-Ag(2)	88.14(14)	O(12)-Ag(1)-Ag(2)	166.26(10)
N(1)-Ag(2)-N(5)	167.08(19)	N(1)-Ag(2)-Ag(1)	83.42(14)
N(5)-Ag(2)-Ag(1)	88.90(14)	C(68)-O(12)-Ag(1)	124.3(4)

Symmetry transformations used to generate equivalent atoms: #1 1-x, 1-y, -z.

DNA-binding studies

Electronic absorption spectra. The DNA-binding experiments were carried out at room temperature. Using the electronic absorption spectral method, the relative bindings of the three complexes to CT-DNA were studied in 5 mM Tris–HCl/50 mM NaCl buffer (pH = 7.2). The solution of CT-DNA gave a ratio of UV absorbance at 260 nm and 280 nm, A_{260}/A_{280}, of 1.8–1.9, indicating that the DNA is sufficiently free of protein [55]. The CT-DNA stock solutions were prepared in 5 mM Tris–HCl/50 mM NaCl buffer, pH = 7.2 (CT-DNA stock solutions were stored at 4 °C and used within 4 days after their preparation). The concentration of CT-DNA was determined from its absorption intensity at 260 nm with a molar extinction coefficient of 6600 M^{-1} cm^{-1} [56].

Absorption titration experiment was performed with fixed concentrations of the complexes (25 μL), while gradually increasing concentration of DNA. When measuring the absorption spectra, an equal amount of DNA was added to both complexes solution (2.5mL Tris-HCl+25μL complexes solution) and the reference solution (2.5mL Tris-HCl+25μL DMF) to eliminate the absorbance of DNA itself. The solutions were allowed to incubate for 5 min before the absorption spectra was recorded. The titration processes were repeated until there was no change in the spectra, indicating binding saturation had been achieved ([complex] = 2.00×10^{-3} mol/L). From the absorption titration data, the binding constant (K_b) was calculated using the equation [39]:

$$[DNA] / (\varepsilon_a - \varepsilon_f) = [DNA] / (\varepsilon_b - \varepsilon_f) + 1/ K_b (\varepsilon_b - \varepsilon_f)$$

Herein, [DNA] is the concentration of CT-DNA in base pairs, ε_a corresponds to the

extinction coefficient observed (A_{obsd} / [M]), ε_f corresponds to the extinction coefficient of the free compound, ε_b is the extinction coefficient of the compound when fully bound to CT-DNA, and K_b is the intrinsic binding constant. The ratio of slope to intercept in the plot of [DNA] / ($\varepsilon_a - \varepsilon_f$) versus [DNA] gives the values of K_b.

Fluorescence spectra. A competitive binding of the complex to CT-DNA lead to the displacement of bound EB or in quenching of the bound EB, and as a consequence the emission intensity of ethidium bromide decreased. In order to further investigate the binding properties of the complex with DNA, competitive binding experiments were performed. The competitive binding experiments were carried out in the buffer by keeping [DNA] / [EB] = 1.14 ([CT-DNA] = 2.50×10^{-3} mol/L, [EB] = 2.20×10^{-3} mol/L) and altering the concentrations of the complexes. The fluorescence spectra of EB were measured using an excitation wavelength of 520 nm and the emission range was set between 550 and 750 nm. The spectra were analyzed based on the classical Stern–Volmer equation [57]:

$$I_0 / I = 1 + K_{sv}[Q]$$

Herein, I_0 and I are the fluorescence intensities at 599 nm in the absence and presence of the quencher, respectively, K_{sv} is the linear Stern–Volmer quenching constant, [Q] is the concentration of the complexes. In these experiments [CT-DNA] = 2.5×10^{-3} mol/L, [EB] = 2.2×10^{-3} mol/L.

Viscosity experiment. Viscosity measurements were carried out on an Ubbelodhe viscometer, immersed in a thermostatic water-bath that maintained at a constant temperature at 25.0 ± 0.1 °C. Titrations were performed for the complexes (3mM), and each complex was introduced into CT-DNA solution (50 μM) present in the viscometer. Data were presented as $(\eta/\eta_0)^{1/3}$ versus the ratio of the concentration of the complex to CT-DNA, where η was the viscosity of CT-DNA in the presence of the complex and η_0 is the viscosity of CT-DNA alone. Viscosity values have been calculated from the observed flow time of CT-DNA containing solution corrected from the flow time of buffer alone (t_0), $\eta = (t-t_0)/t_0$ [58].

Acknowledgement

The present research was supported by the National Natural Science Foundation of China (Grant No. 21367017), Natural Science Foundation of Gansu Province (Grant No. 1212RJZA037).

References

[1] J.J.Perry, J.A.Perman, M.J.Zaworotko, *Chem.Soc.Rev.,* 2009, **38,** 1400-1417.

[2] N.C.Kasuga, A.Sugie, K.Nomiya, *Dalton.Trans.,* 2004, **21**, 3732-3740.

[3] B.Moulton, J.J.Lu, R.Hajndl, S.Hariharan, M.J.Zaworotko, *Angew.Chem.Int.Ed.,* 2002, **41**, 2821-2824.

[4] D.Sun, N.Zhang,.Q.J.Xu, Z.H.Wei, R. B. Huang, L.S.Zheng, *Inorg.Chim.Acta.,* 2011, **368**, 67-73.

[5] L.Hou, D.Li, *Inorg. Chem.Commun.,* 2005, **8**, 128-130.

[6] Y.Cui, C.He, *J. Am. Chem. Soc.,* 2003, **125**, 16202-16203.

[7] D.Sun, C.F.Yang, H.R.Xu, H.X.Zhao, Z.H.Wei, N.Zhang, L.J.Yu, R.B.Huang, L.S.Zheng, *Chem.Commun.,* 2010, **46**, 8168-8170.

[8] M.A.Fik, A.Gorczynski, M.Kubicki, Z.Hnatejko, A.Fedoruk-Wyszomirska, E.Wyszko, M.Giel-Pietraszuk, V.Patroniak. *Eur.J.Med.Chem.,* 2014, **86**, 456-468

[9] X.F.Zheng, L.G.Zhu, *Inorg.Chim.Acta.,* 2011, **365**, 419-429.

[10] D.Venkataraman, Y.H.Du, S.R.Wilson, K.A.Hirsch, P.Zhang, J.S.Moore, *J.Chem.Edu.,* 1997, **74**(8), 915.

[11] F.A.Cotton, G.Wilkinson, *Adv.Inorg.Chem.*, fifthed., Wiley, Chichester, 1988.

[12] K.Chainok, S.M.Neville, C.M.Forsyth, W.J.Gee, K.S.Murray, S.R.Batten, *CrystEngComm.,* 2012, **14**, 3717–3726.

[13] G.K.Kole, C.K.Chin, G.K.Tan, J. J.Vittal, *Polyhedron.,* 2013, **52**, 1440-1448.

[14] M.Boiani, M.González, *Mini-Rev.Med.Chem.,* 2005, **5**, 409-424.

[15] A.Ahmed, E.Rashedy, Y.Hassan, A.Enein, *Curr.Drug.Ther.,* 2013, **8**, 1-14.

[16] K.Kubo, Y.Kohara, Y.Yoshimura, Y.Inada, Y.Shibouta, Y.Furukawa, T.Kato, K.Nishikawa, T.Naka, *J.Med.Chem.,* 1993, **36**(16), 2343-2349.

[17] R.C.Boruah, E.B.Skibo, *J.Med.Chem.,* 1994, **37**(11), 1625-1631.

[18] Y.S.Tong, J.J.Bouska, P.A.Ellis, E.F.Johnson, J.Leverson, X.S.Liu, P.A.Marcotte, A.M.Olson, D.J.Osterling, M.Przytulinska, L.E.Rodriguez, Y.Shi, N.Soni, J.Stavropoulos, S.Thomas, C.K.Donawho, D.J.Frost, Y.Luo, V.L.Giranda, T.D.Penning, *J.Med.Chem.,* 2009, **52**(21), 6803-6813.

[19] Y.F.Li, G.F.Wang, P.L.He, W.G.Huang, F.H.Zhu, H.Y.Gao, W.Tang, Y.Luo, C.L.Feng, L.P.Shi, Y.D.Ren, W.Lu, J.P.Zuo, *J.Med.Chem.,* 2006, **49**(15), 4790-4794.

[20] K.C.S.Achar, K.M.Hosamani, H.R.Seetharamareddy, *Eur.J.Med.Chem.,* 2010, **45**(5), 2048-2054.

[21] C.L.Sann, A.Baron, J.Mann, H.V.D.Berg, M.Gunaratnam, S.Neidle, *Org.Bio.Chem.,* 2006, **4**, 1305-1312.

[22] T.Kálai, M.Balog, A.Szabó, G.Gulyás, J.Jeko, B.Sümegi, K.Hideg, *J.Med.Chem.,* 2009, **52**(6), 1619-1629.

[23] W.W.K.R.Mederski, D.Dorsch, S.Anzali, J.Gleitz, B.Cezanne, C.Tsaklakidis, *Bioorg.Med.Chem.Lett.,* 2004, **14**, 3763-3769.

[24] U.Kalinowska-Lis, A.Felczak, L.Checinska, K.Lisowska and J.Ochocki, *J.Organomet.Chem.,* 2014, **749**, 394-399.

[25] X.X.Wang, Y.G.Liu, K.V.Hecke, A.Goltsev and G.H.Cui, *Z.Anorg.Allg.Chem.,* 2015, **641** (5), 903–910.

[26] J.Hao, B.Yu, K.V.Hecke and G.Cui, *CrystEngComm.,* 2015, **17**,2279.

[27] X.L.Lv, H.Wu, J.F.Ma and J.Yang, *Polyhedron.,* 2011, **30**, 1579–1586.

[28] H.L.Wu, J.K.Yuan, Y.Bai, G.L.Pan, H.Wang, J.Kong, X.Y.Fan and H.M.Liu, *Dalton.Trans.,* 2012,**41**,8829.

[29] H.L.Wu,Y.H.Zhang, C.Y.Chen, J.W.Zhang, Y.C.Bai, F.R.Shi and X.L.Wang, *New.J.Chem.,* 2014,**38**, 3688.

[30] H.Hioki, K.Matsuhita, M.Kubo, K.Harada, M.Kodama and Y.Fukuyama, *Tetrahedron.,* 2007, **63**, 11315-11324.

[31] P.M.Bendale and C.M.Sun, *J.Comb.Chem.,* 2002, **4**(4), 359–361.

[32] M.J. Lin and C.M.Sun, *Synlett.,* 2004(4), 663–666.

[33] M.C. Etter, *Acc.Chem.Res.,* 1990, **23**(4), 120-126.

[34] A.W.Xu, C.Y.Su, Z.F.Zhang, Y.P.Cai, C.L.Chen, *New J.Chem.,* 2001, **25**, 479-482.

[35] L.Yang, D.R. Powell, R.P.Houser, *Dalton Trans.,* 2007, 955–964.

[36] A.W.Addison, T.N.Rao, J.Reedijk, J.van Rijn, G.C.Verschoor, *J.Chem.Soc,Dalton Trans.,* 1984, 1349-1356.

[37] Bo Li, W.K.Wang, S.Q.Zang, T.C.W.Mak, *J.Organomet.Chem.,* 2013, **745-746**, 173-176.

[38] H.L.Wu,Y.C.Gao,*Trans.Met.Chem.,* 2004, **29**(2),175-179.

[39] A.M.Pyle, J.P.Rehmann, R.Meshoyrer, C.V.Kumar, N.J.Turro, N.J. J.K.Barton, *J.Am.Chem.Soc.,* 1989, **111**, 3051-3058.

[40] E.C.Long, J.K.Barton, *Acc.Chem.Res.,* 1990, **23**(9), 271-273.

[41] M.Cory, D.D.McKee, J.Kagan, D.W.Henry, J.A.Miller, *J.Am.Chem.Soc.,* 1985, **107**(8), 2528-2536.

[42] F.J.Meyer-Almes, D.Porschke, *Biochemistry.,* 1993, **32**(16), 4246–4253.

[43] Y.Wang, Z.N. ang, Z.N.Chen, *Bioorg.Med.Chem.Lett.,* 2008, **18**, 298-303.

[44] J.Olmsted, D.R.Kearns, *Biochemistry.,* 1977, **16**(16), 3647-3654.

[45] H.Chao and L.N.Ji, *Bioinorg.Chem.Appl.,* 2005, **3**, 15-28.

[46] B.Peng, H.Chao, B.Sun, H.Li, F.Gao and L.N.Ji, *J.Inorg. Biochem.,* 2007, **101**, 404-411.

[47] M.Chauhan, K.Banerjee, F.Arjmand, *Inorg.Chem.,* 2007, **46**(8), 3072-3082.

[48] S.Satyanarayana, J.C.Dabrowiak, J.B.Chaires, *Biochemistry.,* 1992, **31**(39), 9319-9324.

[49] T.M.Kelly, A.B.Tossi, D.J.McConnell, T.C.Strekas, *Nucleic Acids Res.,* 1985, **13**(17), 6017–6034.

[50] P.T.Selvi, M.Palaniandavar, *Inorg.Chim.Acta.,* 2002, **337**, 420–428.

[51] J.Liu, H.Zhang, C.Chen, H.Deng, T.Lu, L.Ji, *Dalton Trans.,* 2003, 114-119.

[52] H.L.Wu, R.R.Yun, K.T.Wang, K.Li, T.Sao, *Z.Anorg.Allg.Chem.,* 2010, **636**, 629-633.

[53] Bruker, *Smart Saint and Sadabs*, Bruker Axs, Inc., Madison, Wisconsin, USA,

2000

[54] Sheldrick,G.M. *SHELXTL*, Siemmens Analytical X-Ray Instruments, Inc., Madison, Wisconsin, USA, 1996.

[55] J.Marmur, *J.Mol.Biol.,* 1961, **3**, 208-218.

[56] M.E.Reichmann, S.A.Rice, C.A.Thomas, P.Doty, *J.Am.Chem.Soc*. 1954, **76**, 3047-3053.

[57] J.R.Lakowicz, G.Webber, *Biochemistry.,* 1973, **12**(21), 4161-4170.

[58] S.M.Rida, F.A.Ashour, S.El-Haish, M.El-Semary, M.H. Badr, M.A.Shalaby, *Eur.J.Med.Chem.,* 2005, **40**(9), 949-959.